

---

# Saltation Thresholds and Entrainment of Fine Particles at Earth and Martian Pressures

---

Rodman Leach, Ronald Greeley,  
and James Pollack

---

November 1989

(NASA-TM-102193) SALTATION THRESHOLDS AND  
ENTRAINMENT OF FINE PARTICLES AT EARTH AND  
MARTIAN PRESSURES (NASA) 42 p CSCL 03R

N90-14997

Unclas  
63/68 0252159

**NASA**

National Aeronautics and  
Space Administration

1

2

3

4

5

6

7

8

9

10

11

12

---

# **Saltation Thresholds and Entrainment of Fine Particles at Earth and Martian Pressures**

---

Rodman Leach and Ronald Greeley, Dept. of Geology, Arizona State University, Tempe, Arizona  
James Pollack, Ames Research Center, Moffett Field, California

November 1989



National Aeronautics and  
Space Administration

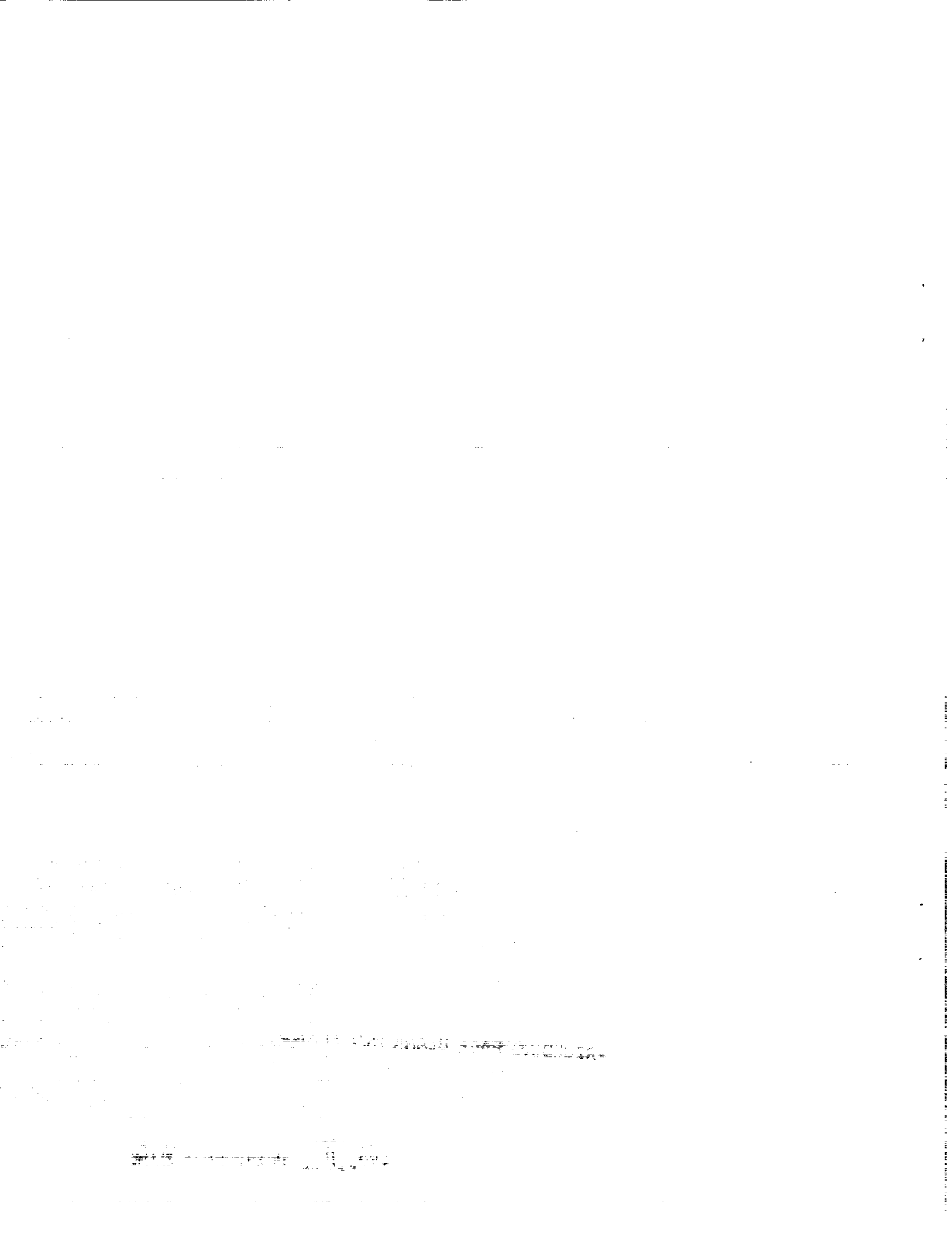
**Ames Research Center**  
Moffett Field, California 94035



# TABLE OF CONTENTS

	Page
SUMMARY .....	1
INTRODUCTION.....	1
WIND TUNNELS.....	2
DESCRIPTION OF TESTS.....	4
Bed Length .....	4
Emplacement of Material.....	4
Threshold Determination.....	5
Measurements.....	5
RESULTS AND DISCUSSION .....	6
Beds of Uniform-Sized Particles.....	6
Beds of Mixed Particle Sizes .....	6
Effects of Surface Roughness .....	6
Fine Particles Bombarded by Saltating Particles .....	7
Effects of Gravity and Interparticle Force.....	8
Agglomerate Particle Threshold.....	8
CONCLUSIONS AND FUTURE WORK .....	9
APPENDIX A – PARTICLES TESTED .....	11
APPENDIX B – ERROR ESTIMATION.....	14
REFERENCES.....	19
TABLES.....	21
FIGURES .....	24

**PRECEDING PAGE BLANK NOT FILMED**



## SUMMARY

An open-circuit wind tunnel designed to operate in a large vacuum chamber was built in 1975 at NASA Ames Research Center to investigate saltation threshold, flux, deflation rates, and other aeolian phenomena on the planet Mars. The vacuum chamber will operate at pressures as low as 4 mbar, and the tunnel operates at windspeeds as high as 150 m/sec. Either air or carbon dioxide can be used as the working fluid. It was found that, to a first-order approximation, the same dynamic pressure was required at martian pressure to entrain or saltate particles as was required on Earth, although wind and particle speeds are considerably higher at martian pressure.

A second wind tunnel, designed to operate aboard the NASA KC-135 0-g aircraft to obtain information on the effect of gravity on saltation threshold and the interparticle force at 0 g, is also described and test data are presented.

Some of the experiments are summarized and various aspects of low-pressure aeolian entrainment for particles 12 to 100  $\mu\text{m}$  in diameter are discussed, some of them unique to low-pressure testing and some common in Earth-pressure particle transport testing. The facility, the modes of operation, and the materials used are described. Although many fundamental questions about aeolian phenomena are answered, the global dust storms observed on Mars have not yet been satisfactorily duplicated or explained with these wind tunnel tests.

## INTRODUCTION

Before the Viking Lander missions to Mars in 1976 it was important to determine what surface wind velocities on Mars cause the large dust storms observed from the Earth. Would such winds be of a magnitude hazardous to the landing of Viking? To answer this and other questions, a Mars Surface Wind Tunnel (MARSWIT, fig. 1) was designed and built at NASA Ames Research Center, and it began operation in 1975. The first question to be addressed was, What minimum surface winds are required to move the optimum-sized particles (i.e., the most easily moved particles), and what is the size of those particles? How much does the required wind velocity increase for particles larger and smaller than the optimum-sized ones?

After the Viking landed, on-board instrumentation measured the surface winds. These measurements indicated surface wind intensities close to those required to move the optimum-sized particles but well below those required for the entrainment of the fine particles observed in the martian atmosphere. Thus it was necessary to gain additional insight into the mechanism of fine-particle entrainment. What is the effect of the lower martian gravity? Does the martian atmosphere, which consists largely of  $\text{CO}_2$ , affect the interparticle force and thus affect the saltation threshold? What is the effect of surface-temperature

gradients on saltation threshold and on particle entrainment into the atmosphere? How does surface roughness affect saltation threshold and flux? What errors does the wind tunnel introduce? These questions have led to further research in MARSWIT and also in the Carousel Wind Tunnel (CWT) which is used to experimentally investigate the effect of gravity and the interparticle force which plays an important role in the aeolian entrainment of fine material. Subsequent tests also addressed the questions of deflation rates, flux, particle velocity, erosion of surface features by windblown material, ripple formation, and other aeolian processes on Mars.

This paper does not address all of these questions, but instead concentrates on those portions of the experiments conducted over the past 15 years that deal with the entrainment of fine particles and the errors that may affect the results obtained. References to other reports that discuss other aeolian matters investigated in MARSWIT are included.

## WIND TUNNELS

MARSWIT is an open-circuit wind tunnel located in a large ( $4058 \text{ m}^3$ ) vacuum chamber that can be evacuated to 4 mbar. The chamber is 30 m high and has a floor area of  $164 \text{ m}^2$ . The tunnel, located centrally in the vacuum chamber (fig. 2), is 13 m long and has a test section 4.8 m long by 1.2 m wide by 0.9 m high. The tunnel is driven by high-pressure air (up to 9.6 bar) ejected through an arrangement of 72 small nozzles located near the exit of the tunnel, providing a maximum velocity of about 140 m/sec at 5 mbar. For most experiments, air is used in the chamber and to drive the tunnel; however, the entire chamber has been filled with  $\text{CO}_2$  for some tests and the tunnel ejectors were driven by  $\text{CO}_2$  at 20 bar, giving a maximum velocity of 150 m/sec at 5 mbar. At an ambient pressure of 1 bar, the tunnel will operate at up to 10.5 m/sec. The tunnel is used primarily for tests of particle threshold, flux, deflation, ripple and bedform evolution, and particle flow around fixed objects.

The entrance to the tunnel has a rectangular-sectioned flow straightener to remove large-scale turbulence. It consists of 88 rectangular openings 10 cm by 10 cm by 25 cm deep. The floor of the tunnel is covered with 700- $\mu\text{m}$  diameter sand particles glued to the floor, from the entry through the test section. The sand is overlaid with 2- to 3-cm pebbles spaced about 10 cm apart for the first 2 m; their function is to add surface roughness to help "trip" the boundary layer, causing an earlier transition from a laminar to a turbulent boundary layer.

Saltation threshold, at which most of the surface particles appear to be bouncing along the bed (saltation < *saltare* (L.), to leap or dance), is detected by three different devices: a laser transmissometer; a particle electrostatic charge detector; and a closed-circuit, high-resolution video system. One or more of these systems is used for each experiment, the effectiveness of each system being dependent on the size and composition of the particles being tested. Particles smaller than about 60  $\mu\text{m}$  in diameter do not saltate but tend to follow the turbulent windstream when they are entrained in the flow.

The transmissometer's laser is located at the front of the tunnel. The laser beam, traversing the length of the tunnel, is reflected back by a mirror at the end of the tunnel and is received by a photo cell located alongside the laser. Thus the beam traverses the bed twice. The mirror is protected by a shield that aerodynamically deflects the particles around the mirror to prevent rapid erosion of the surface. The



beam is located about 2 cm above the surface of the test bed and is most effective for detection of particles of 60 to 600  $\mu\text{m}$ .

The electrostatic saltation detector (ESD) consists of a 50-mm-diameter copper disk mounted on an insulated holder positioned normal to the particle flow. Because moving particles develop a tribocharge (an electrostatic charge resulting from friction), the disk will acquire a charge when it is struck by the particles. This charge is measured as a current on a Keithly electrometer. The particles will obtain both positive and negative charges, depending on their size and composition. The ESD measures the net charge. The ESD has been used to detect motion of particles of 8 to 1200  $\mu\text{m}$ , but is especially effective for the smaller sizes.

The closed-circuit TV system features remote pitch, yaw, and focus. It is valuable for surveying the test bed to determine its condition during runs, and for saltation detection for particles larger than 200  $\mu\text{m}$ . It is essential when monitoring flow deposition and erosion around fixed objects.

The tunnel has undergone extensive calibration with air and  $\text{CO}_2$  at pressures from 1 bar to 4 mbar. (ref. 1).

The CWT is a small, portable wind tunnel used for low-gravity and reduced-pressure tests. It consists of two concentric cylinders constructed of clear Lexan plastic, each 30 cm deep. The the outer cylinder is 60 cm in diameter and the inner cylinder is 40 cm in diameter; the space between the cylinders is the test section (fig. 3). The inner cylinder is spun at speeds of up to 3000 rpm by a variable-speed motor driving a belt-and-pulley arrangement, which causes an airflow between the cylinders. Instrumentation consists of a tachometer, which measures the inner-cylinder rotational speed, and an accelerometer which measures the gravity. The tunnel has been used onboard the NASA KC-135 0-g test aircraft to obtain particle thresholds at 0-1.8 g (ref. 2). This information provided verification of the equations used to correct for the difference between thresholds obtained at Earth gravity and those which would be obtained at martian or other gravity levels. The CWT also provided a convenient means of measuring the interparticle force, which becomes the predominant force resisting entrainment at 0 g. This tunnel has also been used in the vertical gun vacuum chamber (VGCG) to obtain particle thresholds as low as 15 mbar. This capability is especially useful when only a small amount of material is available for testing, because the particles are confined in the closed system and not dispersed outside the tunnel, as is the case with MARSWIT. Threshold information is obtained primarily visually, with videotaping of some of the runs for later analysis.

The CWT was characterized and calibrated with a hot-wire anemometer to obtain the flow characteristics. The friction threshold velocity,  $U_{*t}$ , was obtained by comparing thresholds measured in the CWT for several types and sizes of particles with thresholds obtained in MARSWIT and other tunnels. In the symbol  $U_{*t}$ ,

$$U_* = (\tau/\rho)^{1/2}$$

and  $U_{*t}$  is  $U_*$  at threshold. The symbol  $\tau$  is the drag per  $\text{cm}^2$ , and  $\rho$  is the fluid density;  $\tau$  is a function of the velocity and also of the roughness of the surface over which the wind is flowing, and it can be determined by measuring, with a suitable anemometer, the slope of the wind velocity as a function of

the log of the height above the surface. Conversely, if  $U_{*t}$  is known for a particular particle,  $\tau$  may be determined for a particular wind tunnel by observing the wind velocity at saltation threshold.

## DESCRIPTION OF TESTS

### Bed Length

The length of the test bed is an important parameter in threshold experiments, as the threshold will be higher if the bed is too short. Threshold decreases as bed length increases until a certain critical length is reached, after which further increases in bed length do not affect threshold. This critical length is a function of the tunnel upstream surface, the particle size, and the ambient pressure used during the test, which affects the Reynolds number. A series of threshold experiments was performed early in the testing program, and it was determined that a test-bed length of 200 cm is longer than the critical length required to give minimum and consistent thresholds for all ambient pressures of interest.

### Emplacement of Material

The material to be tested was placed on the floor of the tunnel, usually by pouring the material on the floor and then smoothing it to a uniform depth using a leveling device that is rolled over the bed. This leveling device is a trolley with four small rubber wheels that ride on the tunnel floor on either side of the bed. Several crosspieces connecting the wheels smooth the bed as the trolley traverses the bed length. The resulting bed is about 1 cm deep, 25 cm wide, and 200 cm long. It is located in the center of the test section between the two side walls, with the front of the bed about 5 m from the tunnel entry.

For material less than 40  $\mu\text{m}$  in diameter, the initial threshold may be greatly affected by the method of placement of the material on the tunnel floor (ref. 3). Although this was not known at the time the MARSWIT tests were performed, it fortunately does not affect the low-pressure data obtained, as there is considerable outgassing of entrapped air when the ambient pressure in the tunnel is reduced to martian pressure. This outgassing loosens and redistributes the bed of particles, making bed placement technique far less important. For tests conducted at atmospheric pressure, the initial value of the threshold for particles of under 40  $\mu\text{m}$  is less for a bed that is emplaced by sprinkling the material through a fine sieve than that for a bed emplaced by pouring the material on the floor and smoothing as previously described. However, after the initial threshold has been obtained, the surface is modified by the wind, and the effect of placement is reduced or eliminated. In the low-pressure tests conducted in MARSWIT, the atmospheric threshold was usually obtained both before and after the low-pressure phase. The final values obtained at 1 atm would thus be from a bed that had been modified by both outgassing and wind-distribution of particles. As considerable time is required for outgassing of the finer particles (more time than could be allowed at low pressure during the martian threshold tests), it is necessary to adjust the threshold value upward to account for this (ref. 4). Thresholds were obtained in MARSWIT by starting and stopping the tunnel operation several times under the same condition, gradually increasing the wind velocity until saltation or entrainment was detected by one or more of the three methods described earlier. In nearly every case in MARSWIT, the initial threshold at low pressure is lower than subsequent thresholds. This is attributed to the outgassing effect described earlier, which evidently leaves a few

easily entrained particles on the surface of the bed. After the surface has been modified by the wind, subsequent thresholds are higher (ref. 5).

In some experiments performed with fine material in the CWT, the tunnel was started and stopped a number of times. When the tunnel is stopped, the particles are deposited from suspension or saltation onto the tunnel floor. The thresholds obtained after the particles were deposited in such a manner were reduced compared to the original threshold. This was, however, not a conclusive test, as there are several factors involved. For example, the threshold reduction could be caused by the particles agglomerating to larger sizes during subsequent runs. Also, the particles settle not only on the floor, but also along the vertical portions of the outer wall, where they are more easily entrained because gravity is not holding them to the floor. These more easily moved particles in turn initiate threshold in the main bed of particles. It therefore is not certain that the reduction in threshold was a result of the aeolian placement of the material and not of other factors. It should be noted that the CWT obtains a dynamic rather than a static threshold (ref. 5). This is because in the CWT the particles are confined and they recirculate in the tunnel, the first particles to move initiating the movement of other particles. In MARSWIT, an open-circuit wind tunnel, the particles that saltate are removed from the test as they exit the tunnel.

### Threshold Determination

Threshold is a judgment call—it depends on the observer. It is defined as the windspeed at which *most* of the particles are saltating. For mono-dispersed, uniformly shaped particles, this would cover a relatively small velocity range. However, most particle test beds are not monodispersed, and particle movement from first movement to full threshold covers a large velocity range; thus it is difficult, by visual observations, to ascertain when “most” of the particles are saltating. This range of velocities narrows with decreasing particle size; but for smaller particles, it is also much more difficult to determine when most particles are moving. Instrumented threshold detectors, such as the laser interferometer or the electrostatic charge detector, on which a signal level can be repeated, tend to provide better (more repeatable) threshold data than visual determinations do, but these detectors do not give an indication of the percentage of the surface particles that are moving.

### Measurements

Besides threshold, wind tunnel instrumentation measures ambient pressure and temperature, and total head pressure. Total head pressure is measured by two separate probes—a fixed probe located 20 cm below the tunnel ceiling, and a boundary layer probe that is able to traverse from the floor to a height of 40 cm. The pressure measurements from these two probes are read on separate pressure transducers, and they are compared to each other when the boundary layer probe is sufficiently high above the floor as to be out of the boundary layer and thus reading free-stream pressure. At martian surface pressure the boundary layer is about 14 cm thick at the probe location. Velocity is calculated using the pressures and temperatures measured, and  $U_*$  is determined by the ratio of  $U_*$  to  $U_{free}$  determined by previous boundary layer measurements and calculations, as described earlier (refs. 2 and 6).

## RESULTS AND DISCUSSION

### Beds of Uniform-Sized Particles

Data from the tests done with walnut shell, glass microspheres, basalt, and fly ash are presented in figures 4-7. To a large extent, thresholds obtained at martian atmospheric density follow the same pattern as those obtained at Earth density, with a minimum threshold for particles between 60 and 100  $\mu\text{m}$  in diameter and larger thresholds for both smaller and larger particles. Glass microspheres indicated a minimum threshold for 60- $\mu\text{m}$  particles whereas walnut shell had a minimum value for particles of about 100- $\mu\text{m}$  size. The difference between these two thresholds may be due to a number of factors such as particle shape, density, degree of sorting, moisture content, surface conditions, or electrostatic charge. Only a limited range of thresholds was obtained for fly ash and basalt because the tunnel would not operate at high enough velocities to obtain thresholds at higher pressures. To a first-order approximation, the dynamic pressure for saltation threshold is the same for martian density as for Earth density (fig. 8). Thus

$$U_{\text{Mars}} = U_{\text{Earth}} (\rho_{\text{Earth}}/\rho_{\text{Mars}})^{1/2}$$

since dynamic pressure,  $q$ , is

$$q = 1/2 \rho U^2$$

where  $\rho$  represents the respective atmospheric density, and  $U$  is the free-stream velocity.

### Beds of Mixed Particle Sizes

Beds of particles of mixed particle sizes were tested to determine whether fines would be more easily entrained if mixed with larger particles. One test consisted of preparing a 1:1 mixture by volume of very fine particles (Xerox toner, about 8  $\mu\text{m}$ ), with 100- $\mu\text{m}$  microspheres. These were placed in the usual manner in the test section and the wind was brought to a velocity just above saltation-threshold velocity. The 100- $\mu\text{m}$  microspheres were selectively removed from the bed by the wind, leaving the Xerox toner. Increasing the velocity removed only a few more particles, and it appeared to the eye that finally all the microspheres had been removed. The windspeed could not be raised high enough to move the Xerox toner. This test was performed at both Earth and Mars atmospheric densities, with identical results.

The conclusions reached from these experiments was that with mixtures of near-optimum-sized particles and fines, the optimum-sized particles will saltate, leaving the fines behind. Very few, if any, fines are entrained by this method.

## Effects of Surface Roughness

A second experiment consisted of completely covering a bed of loosely scattered 1-cm pebbles with 100- $\mu\text{m}$  sand particles. This test was conducted in a wind tunnel that duplicates the Venus surface density, with  $\text{CO}_2$  gas used as the working fluid, at 35 bar and room temperature. Initial saltation velocity was the same as that for the sand alone, but the threshold velocity decreased slightly as soon as the pebbles began to be uncovered. The lowered threshold resulted from the roughening of the surface as the pebbles were exposed. Threshold continued to decrease until the pebbles were about half uncovered, and then it began to increase sharply. The point was finally reached when no particles were saltating, even at the highest velocity obtainable, because all the remaining sand was shadowed by the pebbles. The exact geometry of the final bed is dependent upon the amount of pebbles used and the geometry of their spacing (fig. 9).

A similar experiment was conducted in MARSWIT at atmospheric pressure (ref. 7). The experimenter noticed the increase in threshold as the sand bed was deflated, but did not observe the initial decrease in threshold when the bed was partially deflated. This may be because of the very long bed that was used, in which large waves and ripples were formed, or it may be because of the lower Reynolds number of the tests.

It was concluded that there may be some reduction of threshold for near-optimum-sized particles mixed with much larger particles as the effective surface roughness is increased by exposure of the larger particles. This reduction in threshold continues until the more easily moved particles are shielded from the wind by the larger particles, and then threshold increases dramatically.

## Fine Particles Bombarded by Saltating Particles

Another series of tests was conducted in which a bed of sand was placed in front of a bed of fine material such as crushed basalt, with a small separation between the two beds. The purpose of these tests was to use the more easily saltated sand to "kick" the fine material into suspension, a process suggested by Bagnold (ref. 5). The basalt was weighed, and then was placed on a removable portion of the tunnel floor. The original surface area covered by the basalt was measured. The tunnel velocity was then brought to 1.5 times the threshold velocity of the sand, but well below the threshold of the fine material, and thus the sand was caused to saltate across the bed of fine basalt. The basalt bed was monitored by two high-speed motion picture cameras, one looking down on the bed from above and one looking across the bed from the side. A review of the films revealed that incoming sand particles skip across the bed of basalt, kicking up plumes of fines and leaving craters. Most of the fines, however, fall back onto the bed and are not entrained in the airstream. A particle-catcher beside the bed of basalt was used to measure the amount of sand hitting the floor per unit area. By measuring the average area covered by the basalt after the test, and weighing the remnant of basalt, it was possible to determine the mass of basalt removed as a function of the mass of sand bombarding it. Figure 10 shows that this varies from 0.15 to 0.7 gm of basalt per 1 gm of sand. It was concluded that, while this may be a valid mechanism to entrain fine material, it is not a very efficient one unless the wind velocity is near the threshold of the fines. It was expected that a small amount of sand would cause a large amount of fines to

be entrained. Both 200- $\mu\text{m}$  and 500- $\mu\text{m}$  sand was used for the upstream material, and crushed basalt and silicic pumice were used for the fine material.

### **Effects of Gravity and Interparticle Force**

Investigations into the effects of gravity and the interparticle force were also conducted. These tests were carried out aboard the NASA KC-135 0-g test aircraft using the CWT (ref. 6). The tests had two goals: (1) to verify the equations delineating the effect of gravity on threshold and (2) to determine the interparticle force. The advantage of determining the interparticle force at low or 0 g is that interparticle force becomes the predominant force at 0 g. If there were no interparticle force, then as gravity approaches zero, the wind required to entrain material should also approach zero. Thus the wind required at 0 g is a direct function of the interparticle force.

The NASA KC-135 0-g aircraft flies a series of parabolic arcs which produce 0-0.5 g for a 20- to 30-sec period during each maneuver. During pull-up from the parabolic arcs, the gravity level is between 1.8 and 2 g. Up to 50 maneuvers are made during a 3-hr flight, each producing a single saltation-threshold data point.

The tests were conducted in the following manner. The CWT was bolted to the aircraft floor. A video camera was aligned so that the CWT test section, the rpm meter, and an accelerometer measuring the gravity level were all in the field of view. The test material was placed between the drums. The tunnel velocity was brought up to that anticipated for threshold for the programmed gravity level of the maneuver, which was well below the threshold at 1 g. The exact gravity level at which particle movement began was recorded. If the particles did not move because of insufficient wind velocity, or if a higher gravity level was obtained than anticipated, this was noted. A plot of rpm squared versus gravity level for saltation threshold or non-threshold was prepared. A straight line was faired above the non-threshold points and through the lowest points for particle movement, and this was defined as the particle threshold.

Ground walnut shell samples with nominal diameters of 23, 105, 700 and 1,080  $\mu\text{m}$  were tested, as were crushed basalt particles with a 15- $\mu\text{m}$  nominal diameter. The interparticle force as a function of diameter is presented in figures 11 and 12 in table 1.

These values represent the ratio of the velocity required to reach entrainment threshold at 0 g to the velocity required at 1 g. Some of the tests were conducted with a Tesla coil discharging inside the CWT. This technique has been used on various erosion devices in which particles confined to a system become charged and tend to stick to the walls of the devices. Inserting a Tesla coil probe neutralizes the charge on the particles, and the effect is visibly evident as the particles fall from the walls. The Tesla coil did not noticeably reduce the threshold in the CWT tests. Calculations and experiments verify that under many conditions, electrostatic forces are not the predominant interparticle force for the smaller-sized particles (ref. 8).

from a few micrometers in diameter to sub-micrometer size, so it would seem that still higher wind velocities are needed.

Care must be exercised with low-pressure tests of fine material in the wind tunnel, as the outgassing of air or the boil-off of moisture when the ambient pressure is quickly reduced has a lubricating effect which lowers the threshold. Whether some outgassing process could occur on Mars as a result of rapid soil heating from solar radiation is uncertain.

The use of CO<sub>2</sub> gas instead of air does not change the required dynamic pressure needed to initiate entrainment, and it has no apparent effect on the interparticle force.

The effect of the lower martian gravity does not reduce the threshold level for fine particles to the point where the predicted winds on Mars will entrain them from the surface directly.

Bombardment of fines by larger particles is a possible method for entraining fines but it is not an efficient method, and it may have limited application.

Surface roughness reduces threshold velocity only briefly. Soon all the particles are removed from areas of high turbulence and the remaining particles, being shielded from the wind, are not easily moved. Threshold then increases above the threshold for smooth surfaces.

Preliminary MARSWIT experiments indicate that temperature gradients, in which the surface temperature is higher than the air temperature, and thus the boundary layer is unstable, may reduce the velocity required for entrainment as much as 20% and also may increase the amount of material that goes into suspension.

Dust storms on Mars originated in areas other than those observed by the Viking Lander, and winds in those areas may be considerably higher than those observed by Viking. Investigators have theorized that cyclonic winds ("dust devils") may be present on Mars, and these may be responsible for the dust storms observed, although other mechanisms are also possible (refs. 12 and 13). These cyclonic winds could produce high wind velocities over a small area, and may supply the wind velocities the wind tunnel tests indicate are necessary.

Electrostatics are certainly important in the aeolian processes affecting fine particles, both because of the interparticle force resisting entrainment and the role of electrostatics in agglomeration. More study is needed for the determination of the total contribution of electrostatics to the interparticle forces.

The effect of particle shape on threshold also needs more investigation. Plate-like particles such as mica or talc are very difficult to entrain with wind. Entrainment theory usually deals with spherical or nearly spherical particles. Other particle shapes, such as those found in pollens, may have entrainment thresholds quite different from those of spherical particles because of mechanical interparticle forces.

Particle sorting techniques need to be improved. Quantities of particles are usually prepared by sifting them through a series of screens. Dry sifting of fine particles is unsatisfactory because smaller particles cling to the larger particles and may constitute as much as 50% of the sort by mass and many times

## Agglomerate Particle Threshold

Experiments were conducted with naturally formed silt agglomerates. The agglomerates were sorted to a uniform size of 500  $\mu\text{m}$  and the threshold was obtained and compared to that of the unagglomerated silt (see fig. 9). Although the agglomerates were five times the optimum diameter for threshold they were still entrained more easily than the unagglomerated silt was.

Agglomerates may be formed on Earth by various processes. The agglomerates used in these tests were formed by wetting and then drying silt. The resulting cakes were easily broken into nearly spherical agglomerates which were sorted by sifting. Natural agglomerates are sometimes formed by electrostatics, but if they are exposed to the atmosphere they tend to pick up moisture and lose their electrostatic charge, and they are ultimately bound together by molecular, chemical, and capillary forces. Since there is apparently no free water on Mars, there is a question of how long-lasting agglomerates may form on that planet.

Experiments with basalt grains in a paddle wheel erosion device led to a possibly important discovery. Experiments were run to determine the time required to reduce sand-sized particles of basalt to fines by moving them inside the device at martian pressure and martian wind velocities. The material was removed and sized periodically. After several 10-min periods of running, the median size began to increase. It was discovered that very strong electrostatic agglomerates were being formed. These agglomerates were as large as 600  $\mu\text{m}$  and would not pass through a screen when being sorted with a sonic sifter. If they were physically broken apart, they would readily re-form. It was determined by calculation that at the very high-impact speeds at these low pressures (there was very little air in the erosion device to cushion the impact), partial melting at the impact points could occur. It was postulated that minuscule electrets (permanently electrostatically charged areas) (ref. 9) were formed at these melt points, and this would explain why these agglomerates endure so well. Thus a possible mechanism for the formation of long-lasting electrostatic agglomerates under dry martian conditions was revealed (refs. 10 and 11).

The conclusion reached from this research with fines was that one of the most likely ways that fines could be entrained in the martian atmosphere would be that the fines agglomerate into particle sizes which are easily saltated. These agglomerates would be easily broken up by the high-impact forces caused by collision with solid surfaces or with other agglomerates, and the resulting fines would be entrained. Neither mixing sand with fines nor bombarding fines with sand is an efficient method for entraining fines.

## CONCLUSIONS AND FUTURE WORK

Low-pressure threshold tests of various materials in MARSWIT did not yield any surprising results, but rather extended our general knowledge of the subject into the low-pressure range. The dynamic pressure required for particle entrainment is nearly constant from 1 bar down to 4 mbar. Fine particles require large wind velocities for aeolian entrainment. The smallest particles entrained in the MARSWIT facility were 12  $\mu\text{m}$  in diameter, whereas particles observed in the martian atmosphere are believed to be



that percentage by number. Wet sifting improves efficiency but initiates new problems, because the material must be dried and separated.

## APPENDIX A

### PARTICLES TESTED

A brief description of the particles used for the fine-particle aeolian saltation threshold experiments, and the reasons for their use, follows.

#### Ground Nutshell

Ground shells of various nuts, primarily walnut, have been used for aeolian tests. One of the primary reasons for this is that the density of nutshell (1.1 to 1.35 gm/cm<sup>3</sup>) is less than that of sand or basalt. This helps to compensate for the lower gravity on Mars. The shape of a ground shell particle is very much like that of a slightly worn basalt or quartz particle (fig. 14). Nutshell is readily available in pre-sorted sizes—it is used commercially for cleaning carbon from aircraft turbine blades, because it does not erode or damage the blades; this is also an advantage in the wind tunnel, since the nutshell, which is relatively soft, causes minimal abrasion of the tunnel surfaces. Walnut shell was obtained from the Bernard Sirotta Co. of Brooklyn, NY, and from other sources. Tests were conducted with shell particles ranging from 12 to 1,080  $\mu\text{m}$  in diameter (table 2). Walnut shell normally is about 8% moisture by weight. This is both an advantage and a disadvantage. The advantage is that the particles do not have a high electrical resistivity and do not tend to retain an electrostatic charge; therefore, they tend not to form electrostatic agglomerates, and not to have an unduly high interparticle force due to electrostatic charge. The disadvantage of the moisture content becomes manifest in low-pressure testing, in which the moisture, if not partially removed by preheating, causes outgassing of water vapor and fluidization of the test bed for beds of particles of less than 250- $\mu\text{m}$  diameter, and this results in deceptively low threshold readings (ref. 14).

#### Glass Microspheres

Glass microspheres of 5- to 710- $\mu\text{m}$  diameter, in 12 size classes, were tested. Four size ranges are reported on herein (table 2). Glass microspheres were chosen because they have nearly the same density as quartz and are primarily spherical, thus they differ only slightly in these respects from well-rounded sand grains. They were supplied by the Microbeads Division of the Cataphote Corp., Jackson, MI. The materials selected were certified by the supplier to be spheroidal and to contain not more than 15% irregularly shaped particles, not more than 1% sharp angular particles, and not more than 0.5% foreign materials (fig. 15).

Microspheres give reasonably repeatable threshold data, but the smaller sizes retain high electrostatic charges which cause agglomeration.

## Crushed Basalt

Crushed basalt was obtained from the Geology Department at Arizona State University. Crushed basalt has a density of 2.83 gm/cm and is of an angular shape (fig. 16). The size range is 1 to 35  $\mu\text{m}$  with a median size of 16.6  $\mu\text{m}$  (fig. 17). Threshold was achieved in MARSWIT at only a few of the lower pressures tested, with the windspeed available. Most of the tests with basalt involved investigating the process by which the fine material is "kicked" into suspension by being bombarded by more easily moved larger particles located upstream and saltating over the bed. The upstream particles used in these tests were 200- $\mu\text{m}$  and 500- $\mu\text{m}$  quartz sand grains (see Results and Discussion).

Tests were run with this basalt in the CWT, at low gravity, in the KC-135 0-g aircraft, where threshold was obtained from 0 to 1 g.

## Silicic Ash

Silicic ash from Sugar Loaf Mountain, San Francisco Peaks, AZ, was tested in MARSWIT (fig. 18). The ash diameter is between 1.8 and 32  $\mu\text{m}$ , with a median size of 13.5  $\mu\text{m}$  (fig. 19). Threshold was not obtained at the highest windspeed available. When bombarded with 200- $\mu\text{m}$  diameter particles, as described for the basalt beds, the bed of ash was eroded.

## Silt

Initial thresholds were obtained with silt. The silt tested had a diameter of between 2.5 and 50  $\mu\text{m}$ , with a median size of 13.9  $\mu\text{m}$  (figs. 20 and 21). Initial threshold was obtained while there was trapped air outgassing. After a few minutes, the threshold could not be repeated. Thresholds were readily obtained with silt agglomerates. These were naturally occurring agglomerates which were sifted into well-sorted specimens with a median size of 500  $\mu\text{m}$ .

## Fly Ash

Thresholds were obtained with fly ash, which is the fractional product of coal combustion that is carried along with the gases and smoke. It is separated from the smoke by electrostatic precipitators and/or bag houses. The sample tested in MARSWIT consisted mostly of spherical particles 1 to 30  $\mu\text{m}$  in diameter with a median size of 14.8  $\mu\text{m}$  and a density of 2.41 gm/cm<sup>3</sup> (figs. 22 and 23). The fly ash was obtained from the Arapaho Test Facility in Colorado, which is operated by the Electric Power Research Institute of Palo Alto, CA.

## Xerox Toner

Xerox toner is used in the processing of Xerox copies. It consists of thermoplastic spheres, impregnated with carbon black, which are 8  $\mu\text{m}$  in diameter (size information was supplied by the manufacturer). The toner was used in a mixture with fine (100- $\mu\text{m}$ -diameter) sand to determine the threshold of

mixtures of particles. A 1:1 mixture (by volume) was used, and saltation was obtained until almost all of the sand grains had been removed, as determined by visual observation. The toner is black and the sand is white; thus the gray mixture turned black as the sand was removed by the wind. Tests were done at martian pressure and were repeated at a pressure of 1 bar.

### **Quartz Sand**

Quartz sand, purchased from foundry supply houses, was obtained in seven size groups with median size between 100 and 500  $\mu\text{m}$  in diameter (fig. 24). It was not used in fine-particle experiments except as a "kicker" to initiate the movement of fine particles (see Basalt) and in a mix with Xerox toner.

### **Montmorillonite Fractile**

Samples of montmorillonite fractile were supplied by the Jet Propulsion Laboratory (JPL) for saltation tests. Thresholds were obtained in the CWT run in a vacuum chamber. This tunnel was used rather than MARSWIT because only a small quantity of material was available. The montmorillonite was loosely collected into large agglomerates which were not separated for the tests. The agglomerates were between 100 and 1000  $\mu\text{m}$  in diameter, with a median of 490  $\mu\text{m}$ , as determined with a sonic sifter. The deagglomerated sample ranged from 1 to 13  $\mu\text{m}$  in diameter, with a mass median size of 2.7  $\mu\text{m}$  as determined with a Coulter counter (figs. 25 and 26).

### **Copper**

Threshold tests were run with copper particles of nominal size 13  $\mu\text{m}$  in diameter, and density 8.92  $\text{gm}/\text{cm}^3$ . The original purpose of these tests was to determine the effect of particle density and electrostatics on the threshold. Some of the tests were run on an aluminum-foil floor which provided a conducting surface. Another test was conducted with aluminum on both the floor and the ceiling of the tunnel, with a 10-kV potential applied. Neither case showed a significant difference from runs made over a fixed sand floor. The nominal particle size of the copper powder was 13  $\mu\text{m}$ , but there were many agglomerates of between 60 and 120  $\mu\text{m}$ , which greatly influenced the threshold (fig. 27).

## APPENDIX B

### ERROR ESTIMATION

The major factors that have caused variations in threshold measurements in MARSWIT are

1. Measurement errors
  - a. Pressure
  - b. Temperature
  - c. Threshold
  - d. Calibration
2. Particle sorting and sizing
3. Particle agglomeration
4. Moisture content and humidity
5. Bed length
6. Bed emplacement methods
7. Particle shape
8. Electrostatic effects
9. Interparticle forces

Except for (1), it is not correct to call these factors "errors." They are variables that affect threshold, and there are no standard or "correct" values for them. As particle size decreases, all of these factors take on greater importance and cause a greater variance in threshold, except (1c). It is well known that the determination of threshold is subjective—two people looking at the same bed will call threshold at different velocities. This is true even when an aid such as a laser or electrostatic probe is used, although the difference in this case is greatly reduced. This difference is largest with larger particles and smaller with smaller particles, because the difference between first movement and absolute threshold decreases with decreasing particle size.

The velocity equation is

$$V = C(1015 P \cdot T/273 H_0)^{1/2}$$

where

- C = a constant  
P = dynamic pressure, mbar  
H<sub>0</sub> = chamber pressure, mbar  
T = temperature, K

It can be seen that velocity is proportional to the square root of temperature and dynamic pressure and inversely proportional to the square root of chamber pressure. As chamber pressure becomes small, the error in velocity becomes large, with a small error in chamber pressure. This is the most critical factor, since chamber pressure is raised by the air used to drive the tunnel, which exhausts into the

chamber. This becomes most significant at the lowest pressures and the highest velocities, where the most air is ejected.

The easiest way to evaluate errors (1a) to (1c) is to look at the data repeatability for the threshold velocity of a bed of the same materials in alternate tests. Some tests conducted in October 1976 on glass microspheres gave the following results at 5 mbar:

<u>Diameter, <math>\mu\text{m}</math></u>	<u>Repeatability, %</u>
10-5	$\pm 14$
44-74	$\pm 14$
74-149	$\pm 10$
149-250	$\pm 6$
210-420	$\pm 4$
297-590	$\pm 5$
350-710	$\pm 5$

We thus see that repeatability is a function of particle size for this class of materials, and that it is best for the middle-sized particles of 210 to 420  $\mu\text{m}$ .

### **Calibration Errors (1d)**

Calibration errors can be determined by comparing data for a specific material with data obtained in many other wind tunnels for the same material. This has revealed that there is as much as a twofold difference in thresholds obtained for the same material by different investigators. MARSWIT data falls somewhere between the extremes.

### **Particle Sorting and Sizing (2)**

In MARSWIT, there has been a major problem in obtaining or producing uniformly sized materials in the smaller sizes. The limited experimental work that has been done here indicates that particles being of mixed sizes has an important effect on threshold, initial threshold values being influenced by the larger particles in the mixture. Even the determination of particle size is not simple, since different methods use different properties of the materials, and all methods are prone to subtle errors resulting from necessary assumptions.

Most of the particles used in these tests were sorted using dry sieving. While a sieve will not allow particles larger than the mesh openings to pass through, there is no guarantee that smaller particles will pass through. It has been noted that in many cases, up to 50% by mass of sieved material consists of particles smaller than the sieve openings. Small particles cling tenaciously to the larger particles by electrostatic and other interparticle forces. Dry sieving becomes less effective as particle size decreases, and for particles of under 23  $\mu\text{m}$  it is not generally useful.

### **Particle Agglomeration (3)**

Particle agglomeration is most important for the smallest sizes of materials. It is strongly dependent on interparticle forces, especially those resulting from particle humidity and electrostatics. Many agglomerates are originally formed by electrostatics, and then as they pick up moisture they lose their charge but remain held together by the moisture. Other materials form cakes as they adsorb moisture, and these are not easily deagglomerated. It is obvious that if 8- $\mu\text{m}$  particles are agglomerated to 80- $\mu\text{m}$ -diameter agglomerates, the threshold will be greatly affected. It can be difficult to size agglomerates, as they tend to break up with many of the sizing methods used.

### **Moisture Content and Humidity (4)**

Boiling of volatile materials at low pressure (because the boiling point is lower) causes fluidization of the bed and reduces the threshold by up to an order of magnitude (ref. 15). It was determined that as little as 2% moisture by weight can cause boiling. Walnut shell particles were heated to remove moisture before testing. Besides this boiling effect, the direct effect of humidity on threshold caused by particle agglomeration and/or interparticle force needs to be further investigated (refs. 13 and 16).

### **Bed Length (5)**

The effect of bed length on threshold velocity was investigated using three sizes of glass microspheres. It was determined that if a bed length larger than a critical length of 200 cm is used, there is no data error due to variation in bed length.

### **Bed Emplacement Methods (6)**

The importance of bed emplacement methods is just becoming known. The total variation in  $U_{*t}$  due to bed emplacement method can exceed 100% for particles in the 10- $\mu\text{m}$  range in atmospheric-pressure tests. Fortunately, the low-pressure tests in MARSWIT are not affected by bed-emplacement methods. This is because when the chamber is pumped down to martian atmospheric pressure, the air entrapped between the particles is outgassed, and the particles in the bed are loosened and redistributed.

### **Particle Shape (7)**

Particle shape has not been systematically investigated in MARSWIT. Walnut shell was included in the experiments partly because its shape is very similar to that of natural sand.

### **Electrostatic Effects (8)**

There are two ways in which electrostatics may affect the saltation threshold. One is a direct effect in which the electrostatic forces bind particles to each other and to the surface. This interparticle force

may be the predominant force for larger particles, but interparticle forces other than electrostatic predominate for particles less than 15  $\mu\text{m}$  in diameter (ref. 8). The second way in which electrostatic forces affect saltation threshold is by forming fine particles into agglomerates that are more easily moved by the wind (refs. 17 and 18). This may be a very important process on Mars, where long-lasting agglomerates may be formed as a result of a combination of high-speed collisions at low atmospheric densities and very low levels of atmospheric moisture. Most electrostatic effects are difficult to assess, as there are a variety of factors that affect the charging process, and it is difficult to obtain repeatable experimental results.

### **Other Interparticle Forces (9)**

Besides electrostatic forces there are other significant interparticle forces. These include capillary, molecular, and chemical forces, as well as surface roughness and tackiness. These were investigated not in MARSWIT but in CWT. They were tested at low and zero gravity, where the interparticle force is the predominant force resisting saltation for small particles. In these tests the total interparticle force, including electrostatic forces, was obtained. Inaccuracies include errors in determining gravity level and in obtaining a statistically sufficient amount of data.

Capillary interparticle forces may be observed by saltation experiments on particles with different moisture contents. Reference 16 presents data showing the increase of threshold with increased moisture content. Experiments with varying moisture content cannot readily be done at low pressure, because of the "boiling off" of moisture at low pressure.

Chemical effects include salt bonding (ref. 13). Wind tunnel test results may be affected when salt or other chemicals remain on the particles after the moisture has boiled off at low pressure.

The effects of molecular forces and surface roughness have not been investigated here.



## REFERENCES

1. White, B. R.; Leach, R. N.; Iversen, J. D.; and Greeley, R.: Calibration of the MARSWIT Tunnel for Determination of Threshold Speeds. NASA TM-80339, 1979, p. 319.
2. White, B. R.; Leach, R.; Greeley, R.; and Iversen, J. D.: Saltation Experiments Conducted Under Reduced Gravity Conditions. AIAA 25th Aerospace Sciences Meeting, Reno, Nev., 1987.
3. Iversen, J. D.: Particulate Entrainment by Wind. Department Of Aerospace Engineering Project 1699. Iowa State University, 1984.
4. Greeley, R.; Leach, R.; White, B. R.; Iversen, J. D.; and Pollack, J. B.: Threshold Windspeeds for Sand on Mars: Wind Tunnel Simulations. *Geophys. Res. Letters*, vol. 7, 1980, pp. 121-124.
5. Bagnold, R.: *The Physics of Blown Sand and Dunes*. Chapman and Hall, 1971.
6. White, B. R.: Soil Transport by Wind on Mars. *J. Geophys. Res.*, vol. 84, 1979, pp. 4643-4651.
7. Reding, L. M.; Williams, S.; Leach, R.; White, B.; and Greeley, R.: Surface Roughness Effects on Aeolian Processes: Wind Tunnel Experiments. NASA TM-84211, 1981, p. 195.
8. Zimon, A. D.: *Adhesion of Dust and Powder*. Plenum Press, New York, 1969.
9. Moore, A. D.: *Electrostatics and Its Application*. John Wiley, New York, 1973.
10. Krinsley, D. H.; Leach, R.; Greeley, R.; and McKee, T. R.: Simulated Martian Aeolian Abrasion and the Creation of Aggregates. NASA TM-80339, 1979, p. 313.
11. Krinsley, D. H.; Leach, R.; Marshall, J.; and Greeley, R.: Electrostatic Aggregates and Their Physical Properties. NASA TM-82385, 1980, p. 285.
12. Pollack, J. B.; Colburn, D. S.; Flazer, F. M.; Cahn, R.; Carlson, C. E.; and Pidek, D.: Properties and Effects of Dust Particles Suspended in the Martian Atmosphere. *J. Geophys. Res.*, vol. 84, 1979, pp. 2929-2945.
13. Greeley, R.; and Iversen, J. D.: *Wind as a Geological Process*. Cambridge University Press, London, 1985.
14. Greeley, R., White, B. R.; Pollack, J. B.; Iversen, J. D.; and Leach, R.: Dust Storms of Mars: Considerations and Simulations. NASA TM-78425, 1977.
15. Greeley, R.; and Leach, R.: "Steam" Ejection of Dust on Mars: Laboratory Simulation, NASA TM-80339, 1979, p. 304.
16. Pye, Kenneth: *Aeolian Dust and Dust Deposits*. Academic Press, London, 1987.

17. Greeley, R.; and Leach, R.: A Preliminary Assessment of the Effects of Electrostatics on Aeolian Processes. NASA TM-79729, 1978, p. 236.
18. Greeley, R.: Silt-Clay Aggregates on Mars. *J. Geophys. Res.*, vol. 84, pp. 6248-6254.

#### ADDITIONAL SOURCES

1. Greeley, R.; Malone, K.; Leach, R.; Leonard, R.; and White, B. R.: Flux of Windblown Particles on Mars: Preliminary Wind Tunnel Determination. NASA TM-82385, 1980, p. 278.
2. Iversen, J. D.; Pollack, J. B.; Greeley, R.; and White, B. R.: Saltation Threshold on Mars: The Effect of Interparticle Force, Surface Roughness, and Low Atmospheric Density. *Icarus*, vol. 19, 1976, pp. 381-393.
3. Iversen, J. D.; and White, B. R.: Saltation Threshold on Earth, Mars and Venus. *Sedimentology*, vol. 29, 1982, pp. 111-119.
4. Iversen, J. D.; White, B. R.; Greeley, R.; Leach, R.; and Pollack, J. B.: Effect of Interparticle Force and Reynolds Number on Wind Threshold Speed. NASA TM-81776, 1980, p. 228.
5. White, B. R.: A Low Density Boundary-Layer Wind Tunnel Facility. AIAA 25th Aerospace Sciences Meeting, Reno, Nev., 1987.

TABLE 1.— INTERPARTICLE FORCE AS A FUNCTION OF PARTICLE DIAMETER

Particle size, $\mu\text{m}$	Percent of threshold velocity due to interparticle force
15	56
38	50
125	42
700	26
1080	18

TABLE 2.— PARTICLES AND THRESHOLDS

Material	Density, $\text{gm/cm}^3$	Diameter, $\mu\text{m}$	Mass median diameter, $\mu\text{m}$	Friction threshold velocity, <sup>a</sup> $U_{*t}$ cm/sec at 10 mbar air
Silicic pumice	2.2	1.8-32	13.5	--- <sup>b</sup>
Crushed basalt	2.85	3.3-45	16.6	550
Montmorillonite	0.1	1-13	2.7 <sup>c</sup>	140 <sup>d</sup>
Fly ash	2.41	2.8-63	14.8	530
Xerox toner	1	8	8	--- <sup>b</sup>
Ground nutshell	1.1-1.35	--- <sup>b</sup>	12	330
Ground nutshell	1.1-1.35	20-43	39	215
Ground nutshell	1.1-1.35	43-61	51	185
Ground nutshell	1.1-1.35	61-88	74	160
Glass microspheres	2.4-3.0	5-44	--- <sup>b</sup>	275
Glass microspheres	2.4-3.0	44-74	68	220
Glass microspheres	2.4-3.0	53-105	91	230
Glass microspheres	2.4-3.0	74-149	111	260
Silt	2.4	2.5-53	13.9	500
Silt agglomerates	2.4	--- <sup>b</sup>	500	355
Copper powder	8.92	12-200	--- <sup>b</sup>	380
Copper oxide	6.3	--- <sup>b</sup>	8	--- <sup>b</sup>
Silica sand	2.65	200-500	--- <sup>b</sup>	200-300

<sup>a</sup>Actual measured velocity  $\times (C'_f/2)^2$ . This needs to be corrected for outgassing, for temperature, and for  $\text{CO}_2$  gas to obtain martian friction velocity (see ref. 10).

<sup>b</sup>Undetermined.

<sup>c</sup>Agglomerated to 490  $\mu\text{m}$  mass median diameter.

<sup>d</sup>Extrapolated from 15 mbar pressure.

TABLE 3.- WIND TUNNEL TEST RUNS  
(low-pressure MARSWIT tests unless otherwise noted)

Materials used and dates of tests. When multiple runs done on same date, suffix A, B, C added	
Silicic pumice (Sugar Loaf Mountain)	
7/6/87	No threshold obtained
7/7/87	10 mbar with sand in front
Crushed basalt (ASU)	
4/1/77	Basalt from Iversen (no threshold)
1/28/87	With 500- $\mu$ m sand in front
2/10/87	With 200- $\mu$ m sand in front
3/18/87	With 200- $\mu$ m sand in front
4/7/87	Some threshold data at low pressure
5/27/87	Low gravity; KC 135; CWT
7/7/87	15 mbar; VGVC; CWT
7/8/87	15 mbar; VGVC; CWT
7/9/87	15 mbar; VGVC; CWT
7/10/87	15 mbar; VGVC; CWT
8/6/87	CWT; low pressure
10/22/87	With 200- $\mu$ m sand in front
10/27/87 A,B	Movie runs
10/28/87 A,B,C	Movie runs
Montmorillonite fractile particles (JPL)	
5/14/87	CWT
Fly ash (Electric Power Research Inst.)	
4/24/87	
Xerox toner (Xerox)	
3/29/76	No threshold obtained
3/30/76	Toner-and-microsphere mixture; 5 mbar
3/31/76	Toner-and-microsphere mixture; 1 atm
Crushed calcite (Commercial Minerals Co.)	
4/1/76	With fines removed

TABLE 3.- CONCLUDED

Walnut shell (Bernard Sirotta, Inc.)	
7/1/76	12 $\mu\text{m}$
5/27/87	23-35 $\mu\text{m}$ ; low gravity; CWT
4/13/76	20-43 $\mu\text{m}$
4/30/76 B,C	20-43 $\mu\text{m}$
3/1/78	20-43 $\mu\text{m}$ ; CO <sub>2</sub> and air
4/23/76	43-61 $\mu\text{m}$
5/28/76	43-61 $\mu\text{m}$
9/15/77	43-61 $\mu\text{m}$
2/15/78 A	43-61 $\mu\text{m}$ ; CO <sub>2</sub> and air
4/20/76	61-88 $\mu\text{m}$
5/28/76	61-88 $\mu\text{m}$
2/8/78	61-88 $\mu\text{m}$ ; CO <sub>2</sub> and air
Glass microspheres (Cataphote Corp., Jackson, MI)	
3/17/76 A	5-44 $\mu\text{m}$ (size XLX)
10/26/76 B	5-44 $\mu\text{m}$ (size XLX); 4-ft bed
2/9/76	44-74 $\mu\text{m}$ (size L)
2/24/76	44-74 $\mu\text{m}$ (size L)
3/17/76 B	44-74 $\mu\text{m}$ (size L)
10/22/76 A	44-74 $\mu\text{m}$ (size L); 3-m bed
10/22/76 B	44-74 $\mu\text{m}$ (size L); 1.2-m bed
11/5/76	53-105 $\mu\text{m}$ (size ML)
10/21/76 A,B	74-149 $\mu\text{m}$ (size M)
Silt	
5/7/76	Heated, screened
5/11/76	Sifted
6/1/76	Moistened, sifted
6/10/76	
12/1/76	Dried and sifted
3/24/81	Agglomerates
Copper powder	
3/18/76	
3/2/77	On aluminum foil floor; 1 atm
6/21/77	Aluminum on floor and ceiling; 1 atm
Copper oxide powder	
3/19/76	No threshold obtained

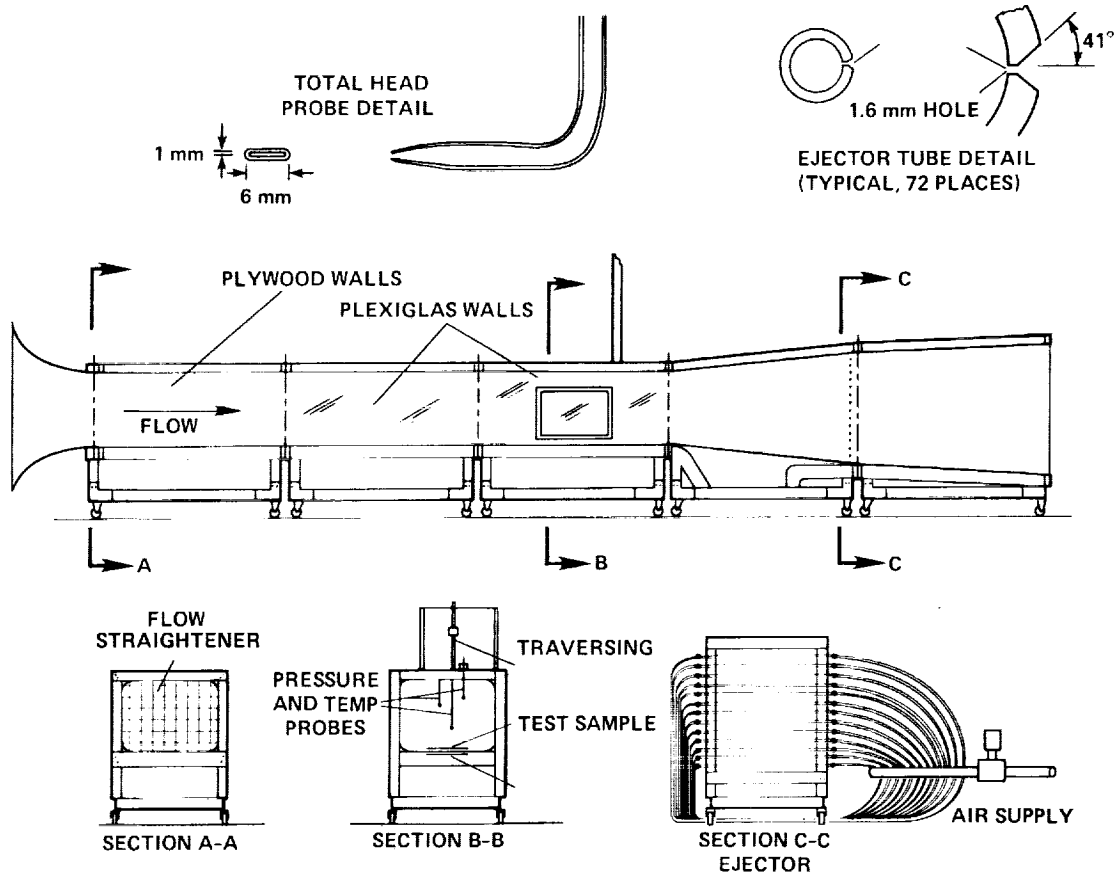


Figure 1.- MARSWIT design details.

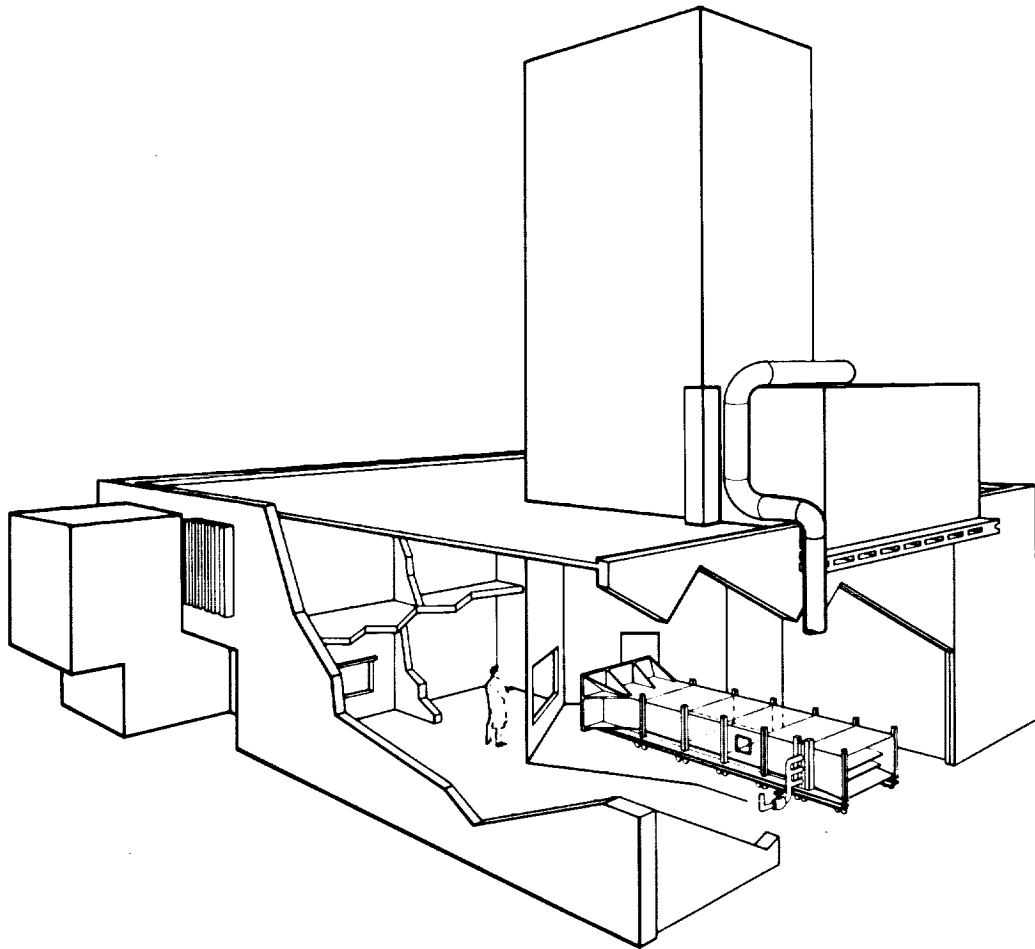


Figure 2.- MARSWIT in vacuum chamber.

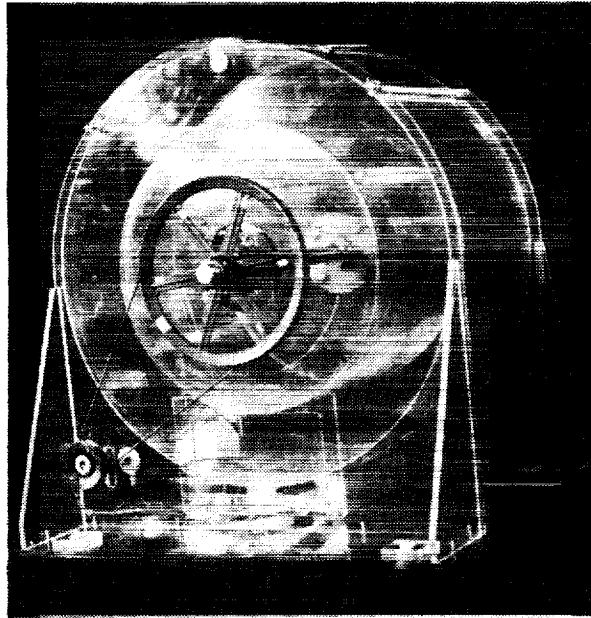


Figure 3.— Carousel Wind Tunnel.

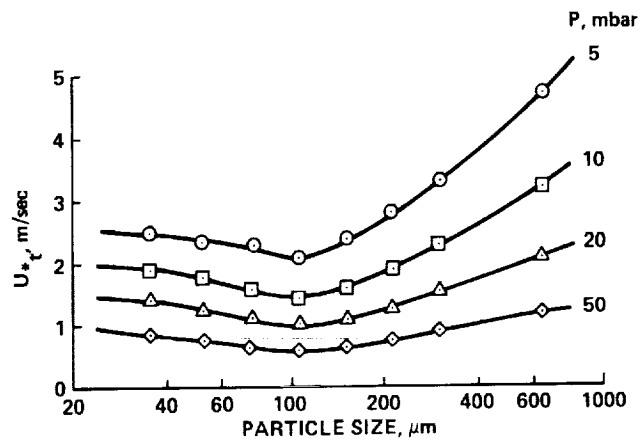


Figure 4.— Walnut shell threshold at low pressure.



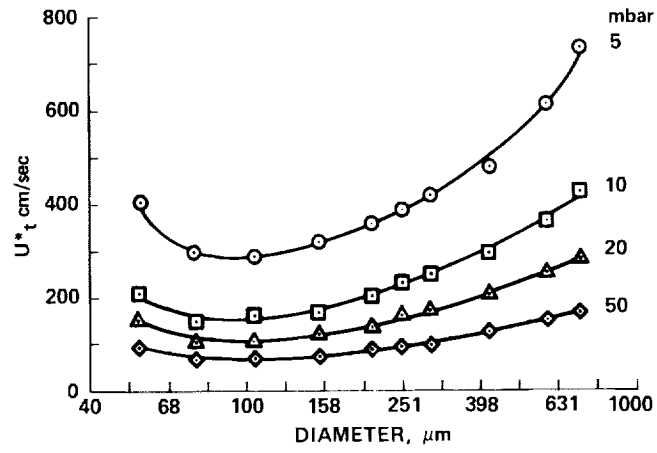


Figure 5.— Microspheres threshold at low pressure.

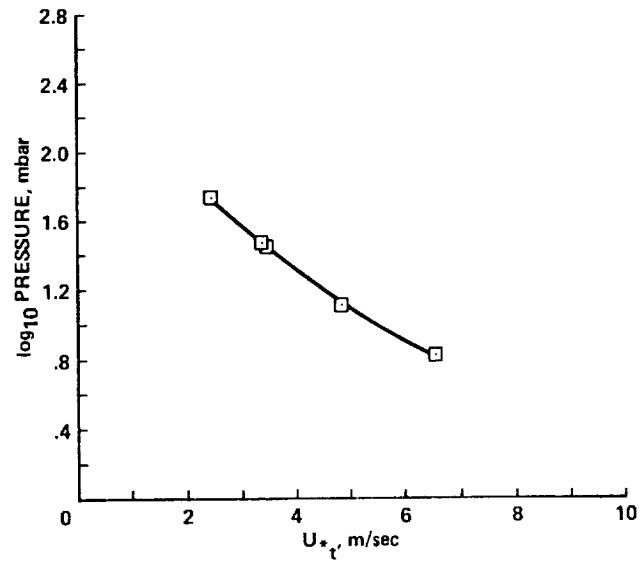


Figure 6.— Basalt threshold at low pressure.

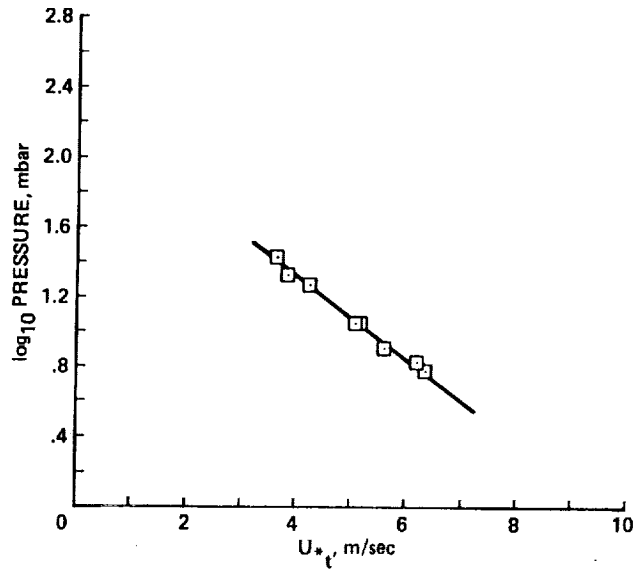


Figure 7.— Fly ash threshold at low pressure.

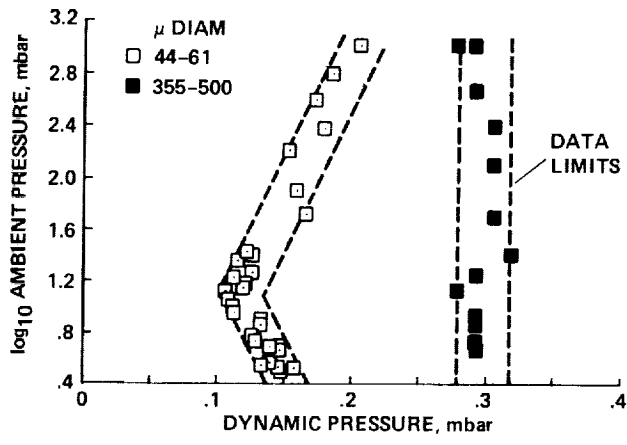


Figure 8.— Threshold dynamic pressure vs. ambient pressure for two sizes of ground walnut shell.

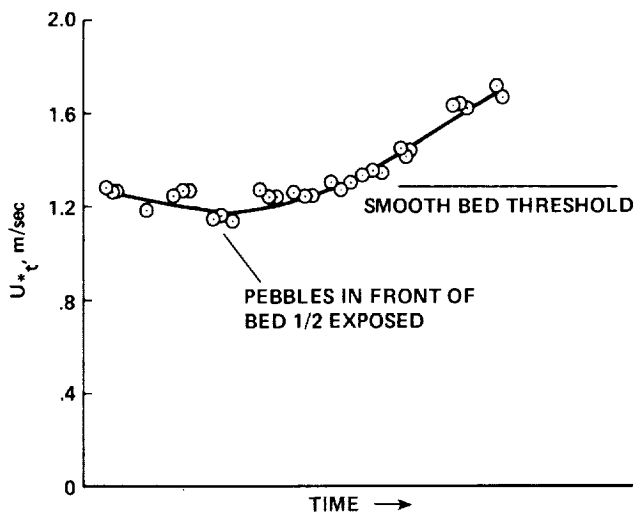


Figure 9.— Threshold of sand and pebble mixture.

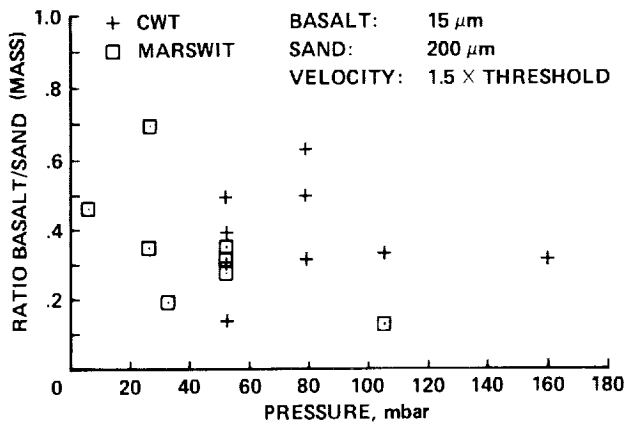


Figure 10.— Effect of sand hitting basalt to initiate entrainment into the airstream.

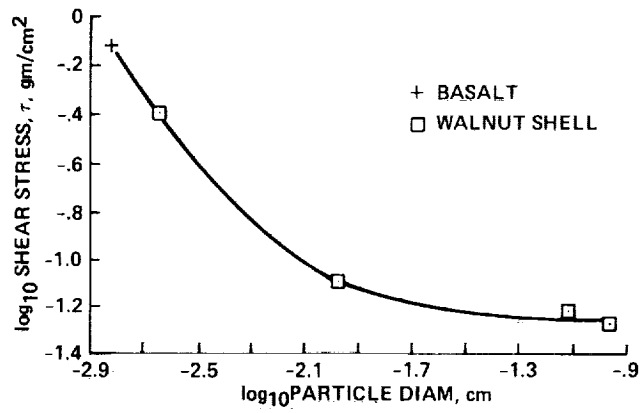


Figure 11.— Interparticle force at 0 g.

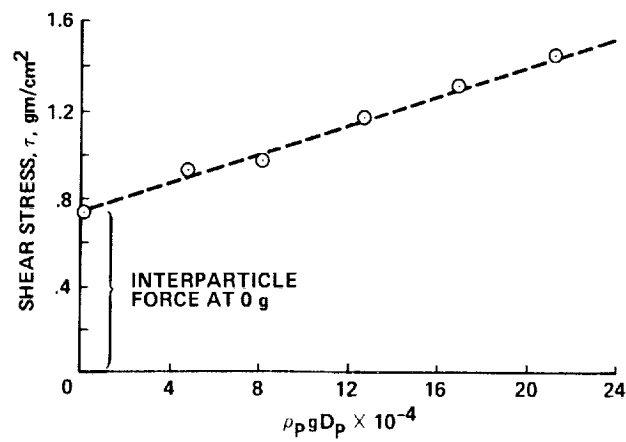


Figure 12.— Basalt interparticle force between 1 and 0 g.

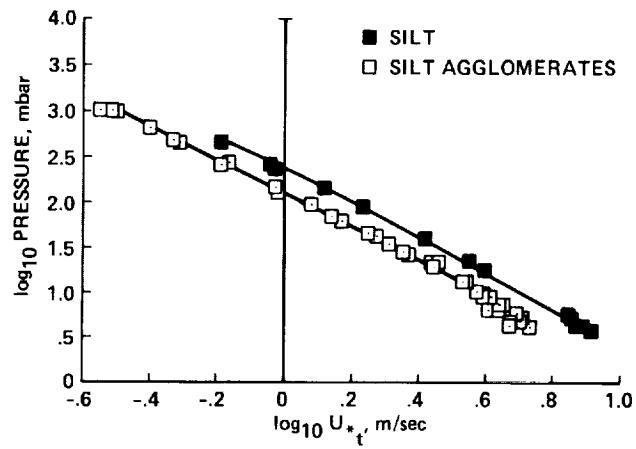


Figure 13.— Silt and silt agglomerate threshold.

ORIGINAL PAGE  
BLACK AND WHITE PHOTOGRAPH

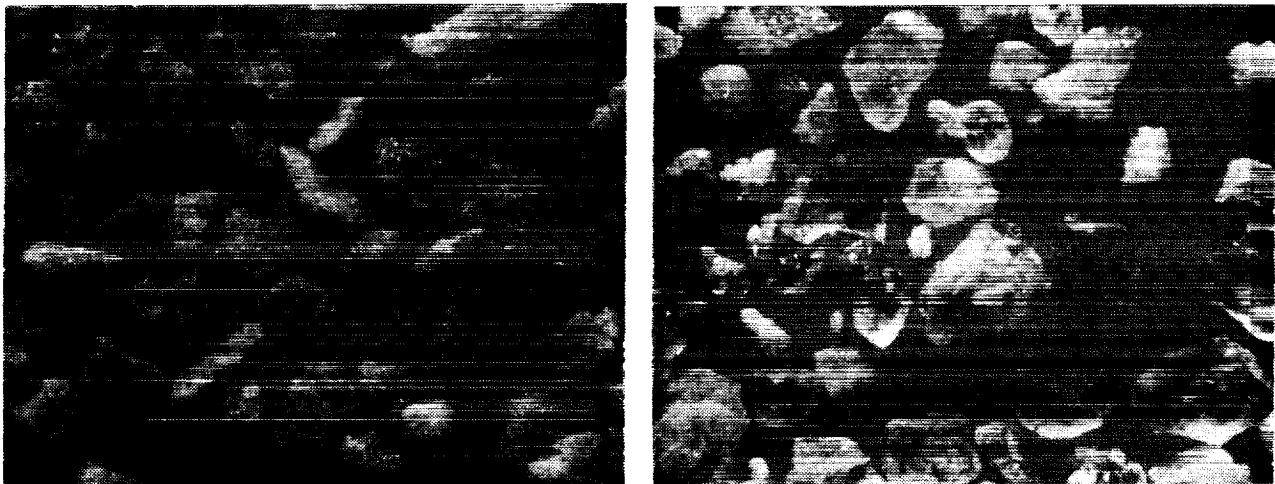


Figure 14.— Ground walnut shell and crushed quartz.

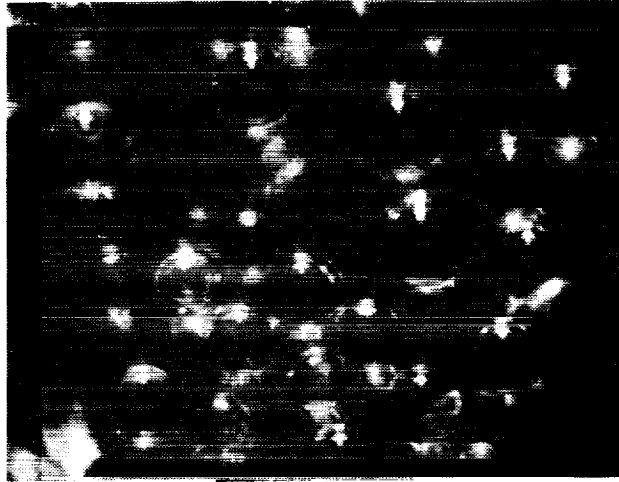


Figure 15.- Glass microbeads (optical microscope).

ORIGINAL PAGE  
BLACK AND WHITE PHOTOGRAPH

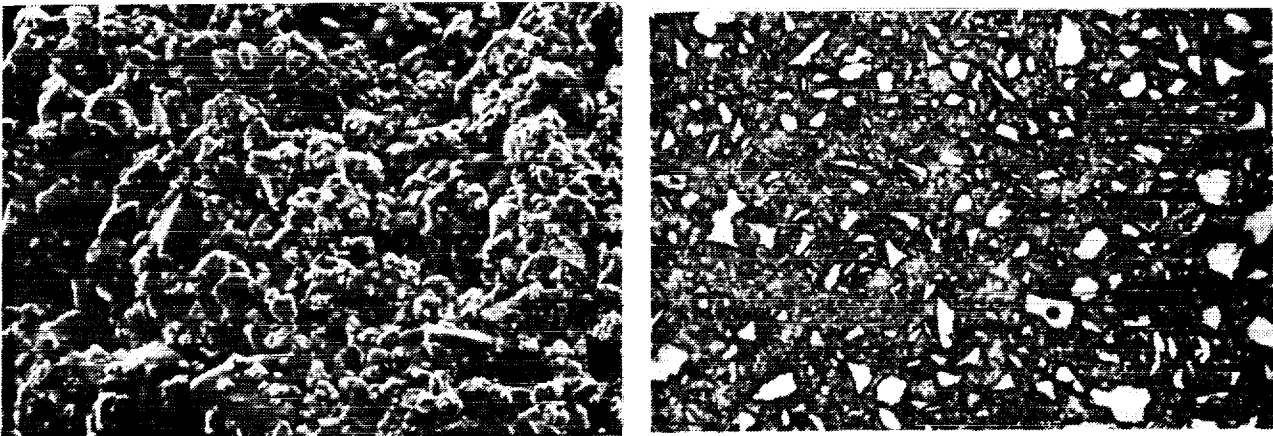


Figure 16.- Crushed basalt (scanning electron microscope (SEM) photograph).

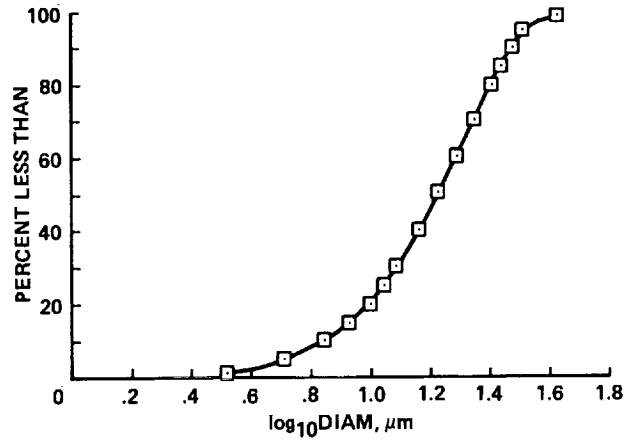


Figure 17.— Basalt size distribution obtained with Coulter counter.

ORIGINAL PAGE  
BLACK AND WHITE PHOTOGRAPH

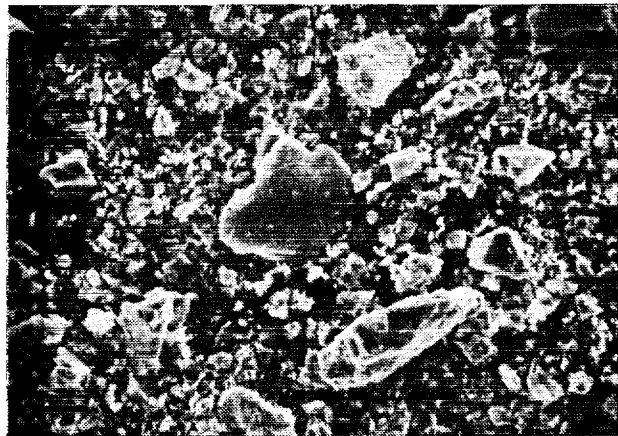


Figure 18.— Silicic pumice ash (SEM photograph).

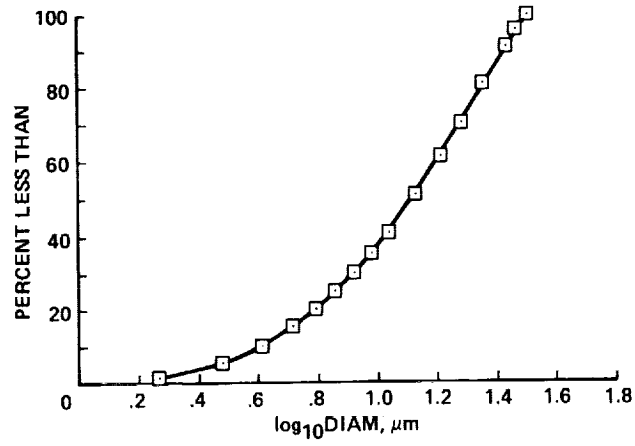


Figure 19.— Silicic pumice ash size distribution obtained with Coulter counter.

ORIGINAL PAGE  
BLACK AND WHITE PHOTOGRAPH

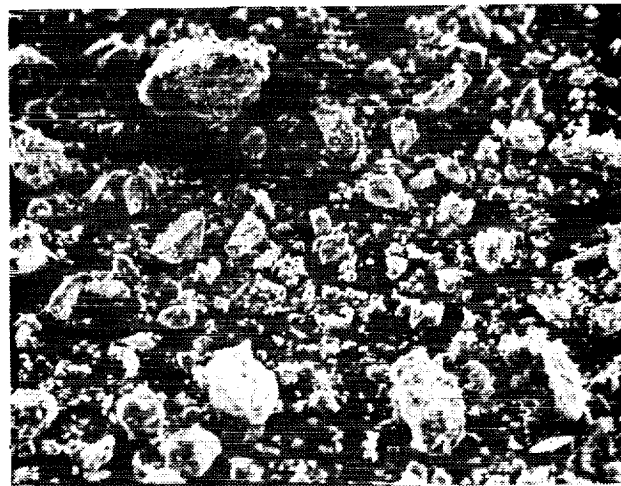


Figure 20.— Silt (SEM photograph).



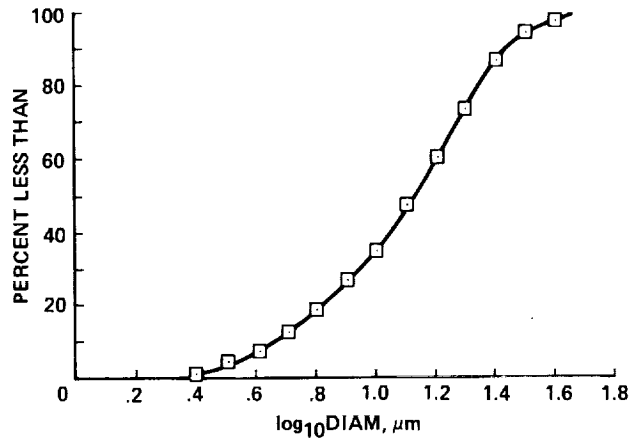


Figure 21.— Silt size distribution obtained with Coulter counter.

ORIGINAL PAGE  
BLACK AND WHITE PHOTOGRAPH

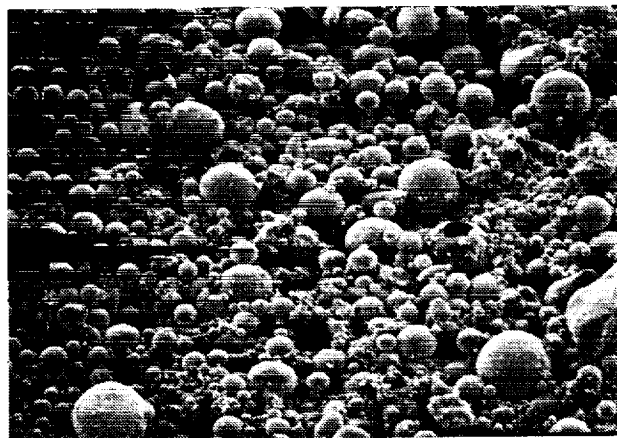


Figure 22.— Fly ash (SEM photograph).

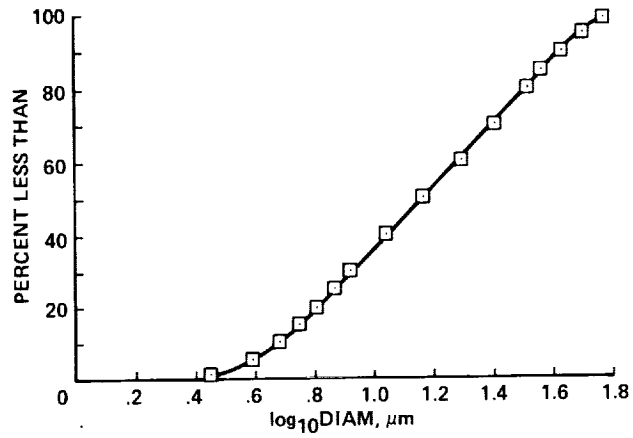


Figure 23.— Fly ash size distribution obtained with Coulter counter.

ORIGINAL PAGE  
BLACK AND WHITE PHOTOGRAPH

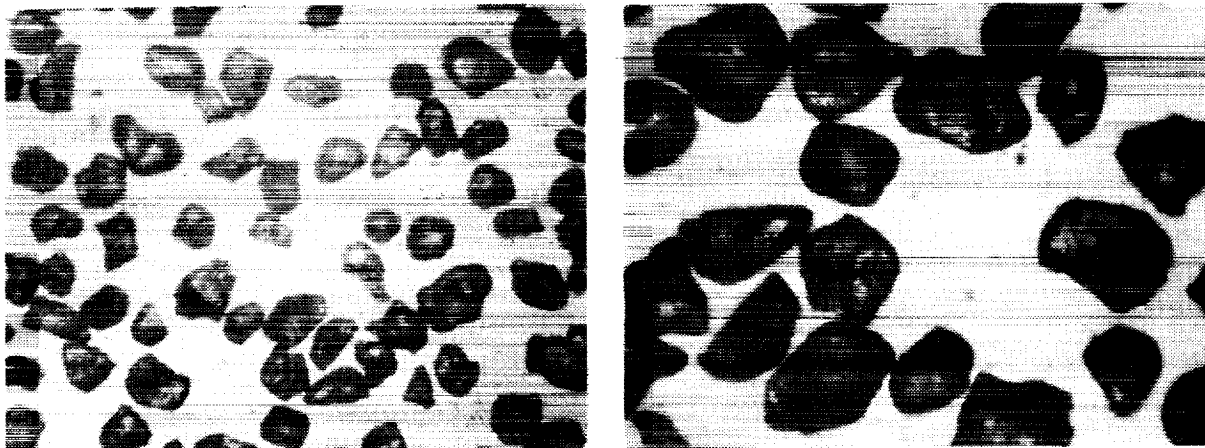


Figure 24.— Quartz sand (optical microscope photograph).

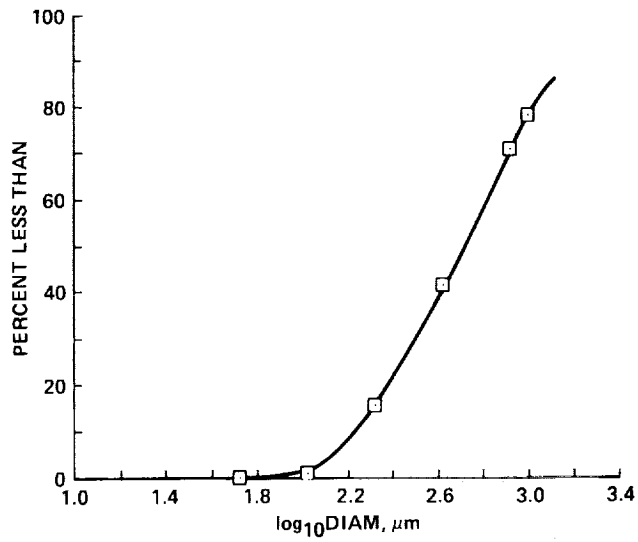


Figure 25.— Montmorillonite agglomerate size distribution obtained with sonic sifter.

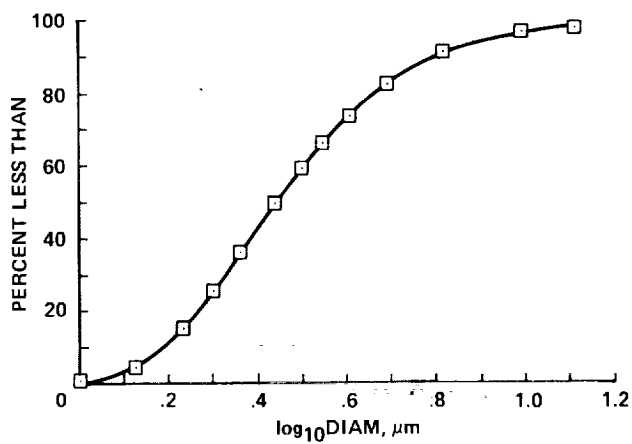


Figure 26.— Montmorillonite size distribution obtained with Coulter counter.

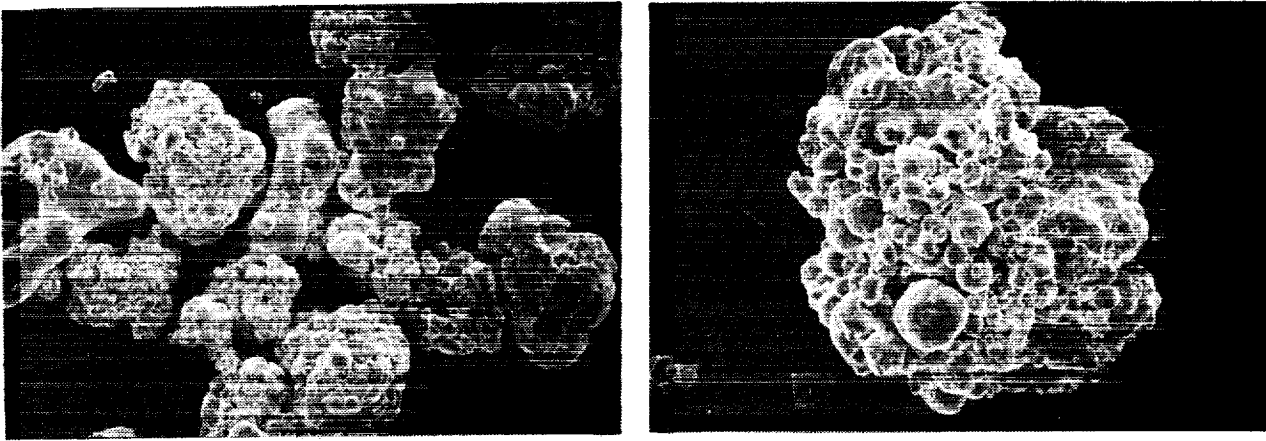


Figure 27.— Copper particles (SEM photograph).

ORIGINAL PAGE  
BLACK AND WHITE PHOTOGRAPH



# Report Documentation Page

1. Report No. NASA TM-102193		2. Government Accession No.		3. Recipient's Catalog No.	
4. Title and Subtitle Saltation Thresholds and Entrainment of Fine Particles at Earth and Martian Pressures			5. Report Date November 1989		
			6. Performing Organization Code		
7. Author(s) Rodman Leach and Ronald Greeley (Dept. of Geology, Arizona State University, Tempe, Arizona), and James Pollack			8. Performing Organization Report No. A-89136		
			10. Work Unit No.		
9. Performing Organization Name and Address Ames Research Center Moffett Field, CA 94035			11. Contract or Grant No. NCC 2-346		
			13. Type of Report and Period Covered Technical Memorandum		
12. Sponsoring Agency Name and Address National Aeronautics and Space Administration Washington, DC 20546-0001			14. Sponsoring Agency Code		
			15. Supplementary Notes Point of Contact: James Pollack, Ames Research Center, MS 245-3, Moffett Field, CA 94035-1000 (415) 694-5530 or FTS 464-5530		
16. Abstract <p>An open-circuit wind tunnel designed to operate in a large vacuum chamber was built in 1975 at NASA Ames Research Center to investigate saltation threshold, flux, deflation rates, and other aeolian phenomena on the planet Mars. The vacuum chamber will operate at pressures as low as 4 mbar, and the tunnel operates at windspeeds as high as 150 m/sec. Either air or carbon dioxide can be used as the working fluid. It was found that, to a first-order approximation, the same dynamic pressure was required at martian pressure to entrain or saltate particles as was required on Earth, although wind and particle speeds are considerably higher at martian pressure.</p> <p>A second wind tunnel, designed to operate aboard the NASA KC-135 0-g aircraft to obtain information on the effect of gravity on saltation threshold and the interparticle force at 0 g, is also described and test data are presented.</p> <p>Some of the experiments are summarized and various aspects of low-pressure aeolian entrainment for particles 12 to 100 <math>\mu\text{m}</math> in diameter are discussed, some of them unique to low-pressure testing and some common in Earth-pressure particle transport testing. The facility, the modes of operation, and the materials used are described. Although many fundamental questions about aeolian phenomena are answered, the global dust storms observed on Mars have not yet been satisfactorily duplicated or explained with these wind tunnel tests.</p>					
17. Key Words (Suggested by Author(s)) Fine particle entrainment, Low-pressure wind tunnel tests, Martian pressure wind tunnel tests, Saltation thresholds			18. Distribution Statement Unclassified-Unlimited  Subject Category - 88		
19. Security Classif. (of this report) Unclassified		20. Security Classif. (of this page) Unclassified		21. No. of Pages 43	22. Price A04

